Robust Control of Rigid Rotor Active Magnetic Bearing System Based on Signal Compensation

Yichen Yao[1]*, Yixin Su[2]†, Tianye Yu[3]‡, Honglei Sha[4]§ and Suyuan Yu[5]¶

[1] Department of Energy and Power Engineering, Tsinghua University, Beijing, 100084, P. R. China.
`yaoyc18@mails.tsinghua.edu.cn`
[2] Department of Energy and Power Engineering, Tsinghua University, Beijing, 100084, P. R. China.
`syx16@mails.tsinghua.edu.cn`
[3] Tianjin Emaging Technology Co. Ltd,Tianjin, 300457, P. R. China.
`yutianye@emaging.com.cn`
[4] Tianjin Emaging Technology Co. Ltd,Tianjin, 300457, P. R. China.
`amb@emaging.com.cn`
[5] Department of Energy and Power Engineering, Tsinghua University, Beijing, 100084, P. R. China.
`suyuan@mail.tsinghua.edu.cn`

Abstract

Active magnetic bearings (AMBs) use the controlled magnetic force to achieve frictionless relative motion between the stator and the rotor. In the case of a large operating speed range, the gyroscopic effect, the unbalance force, the unmodeled dynamics and disturbances in the rotor-AMBs system has become a non-negligible factor that may influence the stability and the dynamic behavior of the system. To avoid this problem, robust control methods based on signal compensation are applied to design the controllers of the rotor-AMBs system in this paper. Firstly, the rigid rotor-AMBs system is described with lumped uncertainties under sensor general coordinates system. On the basis of the model, the control system is designed. The control system contains nominal controllers and compensators. The target of the nominal controller is to stabilize the nominal part of the system. The robust compensator aims to generate the compensation signal to suppress the lumped uncertainties equivalent disturbance robustly. According to the design, we have done laboratory experiments on an AMB-supported industrial permanent magnet synchronous motor (PMSM). The results show that the design method based on signal compensation has good performance.

1 Introduction

Active magnetic bearings (AMB) is widely used in rotating machinery because of its advantages of no friction, no lubrication or sealing requirements, long lifespan, low maintenance and active vibration control [11, 12, 14]. However, the design of magnetic bearing controller relies on accurate rotor-AMBs system modeling as well as precise external disturbance modeling, which restrict the industrial application and popularization of magnetic bearing. In fact, the AMB controller often requires a long time to adjust related parameters while in operation.

In recent years, many researches have focused on AMB controller design in order to achieve better vibration suppression performance and improve the robustness of the controller. As

---

*Proposed the idea and designed the controller.
†Did numerous tests and provided a lot of suggestions.
‡Helped establish the test rig.
§Helped adjust the test rig and the control parameters.
¶Guided the research and provided a lot of suggestions.

for vibration suppression, plentiful good controllers have been proposed. Shiqiang Zheng et al. [2] proposed a feed-forward control strategy combined with a novel adaptive notch filter to solve the rotor unbalance problem in magnetic suspended centrifugal compressors. To the same problem, Qi Chen, et al. [1] put forward a double-loop compensation design approach based on the AMBs. Fang et al. [4] designed a gain phase modifier to compensate the gain and phase errors caused by the power amplifier and completely achieved automatic balance of the rotor. Zhang Kai, et al. [8] designed a comprehensive controller for the AMBs on a turbo molecular pump, using different methods to suppress different kinds of vibration. Jiang et al. [6] realized multi-frequency periodic vibration suppressing in active magnetic bearing-rotor systems through response matching in frequency domain. However, the premise of good performance of these controllers is the exact model of the external forces and the system model.

To achieve enough robustness, adaptive control strategy, robust control strategy, active disturbance rejection strategy and many other methods have been applied on AMBs. Dhyani et al.[3] applied heuristic moth-flame optimization algorithm to optimize the scaling factors of the fuzzy-PID controller in a AMBs system. Under this algorithm, the AMBs showed great robustness to external periodic excitations and step input. Su et al. [13] proposed a PID-surface sliding mode control method, which possessed high tracking accuracy and anti-jamming capacity. In [10], an adaptive back-stepping control based on sliding mode approach is applied to a linearized model of an active magnetic bearing system in order to deal with the external disturbance. In [7] and [5], an PID controller with extended state observer (ESO) is applied on decentralized control of AMB-rotor system and corresponding experiments have been performed. In [9], an robust controller with feedback-linearization ESO is employed on a MSCMGs system and achieves good performance. However, these controllers have relatively more complex structure and the parameters adjustment procedure.

This paper proposes a robust controller based on signal compensation. It contains a PD controller as nominal controller and a simple-structure robust compensator. Corresponding experimental verification has been carried out on an industrial AMB-supported permanent magnet synchronous motor (PMSM) test rig. The proposed strategy is compared with a PID controller with the same nominal controller. The results show that the proposed control strategy is effective.
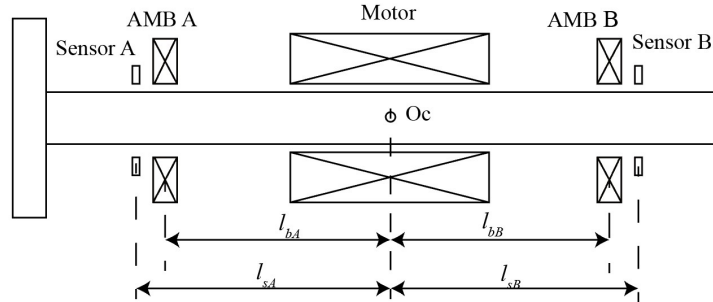
2 System modeling

Figure 1: Structure of the AMB-rigid rotor system.

The structure of the AMB-rigid rotor system is shown in Fig.1. The terms x_c, y_c represent rotor's centroid's displacement; α, β are the rotor's angular displacement around x and y axes. The terms $l_{bA}, l_{bB}, l_{sA}, l_{sB}$ show the distance between the A/B bearing/sensor and the centroid. In AMB-rigid rotor system, the coupling between the axial DOF and radial DOF is negligible. Thus, axial DOF is not mentioned in this model and merely radial 4 DOF and axial angle γ are considered. There are three coordinates to illustrate the motion of rotor, which are centroid coordinate $\mathbf{y}^c = \begin{bmatrix} x_c & \alpha & y_c & \beta \end{bmatrix}^T$, sensor coordinate $\mathbf{y}^s = \begin{bmatrix} y_{Ax}^s & y_{Ay}^s & y_{Bx}^s & y_{By}^s \end{bmatrix}^T$, and bearing coordinate $\mathbf{y}^b = \begin{bmatrix} y_{Ax}^b & y_{Ay}^b & y_{Bx}^b & y_{By}^b \end{bmatrix}^T$. The relation between them can be expressed as $\mathbf{y}^s = \mathbf{T}^{sc}\mathbf{y}^c, \mathbf{y}^c = \mathbf{T}^{cb}\mathbf{y}^b$, in which

$$
\mathbf{T}^{cb} = \begin{bmatrix} 1 & 0 & 1 & 0 \\ 0 & -l_{bA} & 0 & l_{bB} \\ 0 & 1 & 0 & 1 \\ l_{bA} & 0 & -l_{bB} & 0 \end{bmatrix}
$$

$$
\mathbf{T}^{sc} = \begin{bmatrix} 1 & 0 & 0 & l_{sA} \\ 0 & -l_{sA} & 1 & 0 \\ 1 & 0 & 0 & -l_{sB} \\ 0 & l_{sB} & 1 & 0 \end{bmatrix}
$$

The bearing force is defined as $\mathbf{f}_b^b = \begin{bmatrix} f_{bAx} & f_{bAy} & f_{bBx} & f_{bBy} \end{bmatrix}^T$, with the load defined as $\mathbf{f}_g^c = \begin{bmatrix} f_{gx}^c & f_{g\alpha}^c & f_{gy}^c & f_{g\beta}^c \end{bmatrix}^T$. According to the second Lagrange equation, the equation of motion (EOF) of the rotor is obtained:

$$
\begin{cases} m\ddot{x}_c = f_{bAx} + f_{bBx} + f_{ex}^c + f_{gx}^c \\ J_r\ddot{\alpha} + J_z\dot{\gamma}\dot{\beta} = -l_{bA}f_{bAy} + l_{bB}f_{bBy} + f_{e\alpha}^c + f_{g\alpha}^c \\ m\ddot{y}_c = f_{bAy} + f_{bBy} + f_{ey}^c + f_{gy}^c \\ J_r\ddot{\beta} - J_z\dot{\gamma}\dot{\beta} = l_{bA}f_{bAx} - l_{bB}f_{bBx} + f_{e\beta}^c + f_{g\beta}^c \end{cases} \tag{1}
$$

where the unbalance force can be rewritten in vector form

$$
\mathbf{f}_e^c = \begin{bmatrix} f_{ex}^c \\ f_{e\alpha}^c \\ f_{ey}^c \\ f_{e\beta}^c \end{bmatrix} = \dot{\gamma}^2 \begin{bmatrix} -me_y & me_x \\ -J_{\mathrm{xz}} & -J_{\mathrm{yz}} \\ me_x & me_y \\ -J_{\mathrm{yz}} & J_{\mathrm{xz}} \end{bmatrix} \begin{bmatrix} \sin\gamma \\ \cos\gamma \end{bmatrix}
$$

Transform (1) to sensor coordinate yields (2)

$$
\begin{cases} \ddot{y}_{Ax}^s = -\frac{J_z\Omega l_{sA}}{J_r(l_{sA}+l_{sB})}\left(\dot{y}_{Ay}^s - \dot{y}_{By}^s\right) + \left(\frac{1}{m} + \frac{l_{bA}l_{sA}}{J_r}\right)f_{bAx} + \left(\frac{1}{m} - \frac{l_{sA}l_{bB}}{J_r}\right)f_{bBx} + f_{eAx}^s + f_{gAx}^s \\ \ddot{y}_{Ay}^s = -\frac{J_z\Omega l_{sA}}{J_r(l_{sA}+l_{sB})}\left(\dot{y}_{Bx}^s - \dot{y}_{Ax}^s\right) + \left(\frac{1}{m} + \frac{l_{bA}l_{sA}}{J_r}\right)f_{bAy} + \left(\frac{1}{m} - \frac{l_{sA}l_{bB}}{J_r}\right)f_{bBy} + f_{eAy}^s + f_{gAy}^s \\ \ddot{y}_{Bx}^s = -\frac{J_z\Omega l_{sB}}{J_r(l_{sA}+l_{sB})}\left(\dot{y}_{By}^s - \dot{y}_{Ay}^s\right) + \left(\frac{1}{m} - \frac{l_{bA}l_{sB}}{J_r}\right)f_{bAx} + \left(\frac{1}{m} + \frac{l_{bB}l_{sB}}{J_r}\right)f_{bBx} + f_{eBx}^s + f_{gBx}^s \\ \ddot{y}_{By}^s = -\frac{J_z\Omega l_{sB}}{J_r(l_{sA}+l_{sB})}\left(\dot{y}_{Ax}^s - \dot{y}_{Bx}^s\right) + \left(\frac{1}{m} - \frac{l_{bA}l_{sB}}{J_r}\right)f_{bAy} + \left(\frac{1}{m} + \frac{l_{bB}l_{sB}}{J_r}\right)f_{bBy} + f_{eBy}^s + f_{gBy}^s \end{cases} \tag{2}
$$

The rotor centroid's precise position is difficult to determine due to its complex shape and its heterogeneous material, which indicate (2) has uncertainty. This uncertainty can be regarded as contained in $\mathbf{f}_g$.

As for AMBs, no matter what control strategy is applied, the bearing force can always be considered as the expected control force generated by a specific controller:

$$f_{bn} \approx u_n, \quad n = Ax, Ay, Bx, By \tag{3}$$

where u_n is the expected control force.

So that (2) can be rewritten as (4). In (4), each sensor coordinate's differential equation is decoupled formally and the plant model of the decentralized controller can be obtained from this.

$$\begin{cases} \ddot{y}_{Ax}^s = \left(\frac{1}{m} + \frac{l_{bA}l_{sA}}{J_r} \right) u_{Ax} + d_{Ax} \\ \ddot{y}_{Ay}^s = \left(\frac{1}{m} + \frac{l_{bA}l_{sA}}{J_r} \right) u_{Ay} + d_{Ay} \\ \ddot{y}_{Bx}^s = \left(\frac{1}{m} + \frac{l_{bB}l_{sB}}{J_r} \right) u_{Bx} + d_{Bx} \\ \ddot{y}_{By}^s = \left(\frac{1}{m} + \frac{l_{bB}l_{sB}}{J_r} \right) u_{By} + d_{By} \end{cases} \tag{4}$$

In (4), d represents the static coupling (coupling of u) and the dynamic coupling (coupling of ,which means the gyroscopic effect), the specific expression is

$$\begin{cases} d_{Ax} = \left(\frac{1}{m} - \frac{l_{sA}l_{bB}}{J_r} \right) u_{Bx} - \frac{J_z\Omega l_{sA}}{J_r(l_{sA}+l_{sB})} \left(\dot{y}_{Ay}^s - \dot{y}_{By}^s \right) + f_{eAx}^s + f_{gAx}^s \\ d_{Ay} = \left(\frac{1}{m} - \frac{l_{sA}l_{bB}}{J_r} \right) u_{By} - \frac{J_z\Omega l_{sA}}{J_r(l_{sA}+l_{sB})} \left(\dot{y}_{Bx}^s - \dot{y}_{Ax}^s \right) + f_{eAy}^s + f_{gAy}^s \\ d_{Bx} = \left(\frac{1}{m} - \frac{l_{bA}l_{sB}}{J_r} \right) u_{Ax} - \frac{J_z\Omega l_{sB}}{J_r(l_{sA}+l_{sB})} \left(\dot{y}_{By}^s - \dot{y}_{Ay}^s \right) + f_{eBx}^s + f_{gBx}^s \\ d_{By} = \left(\frac{1}{m} - \frac{l_{bA}l_{sB}}{J_r} \right) u_{Ay} - \frac{J_z\Omega l_{sB}}{J_r(l_{sA}+l_{sB})} \left(\dot{y}_{Ax}^s - \dot{y}_{Bx}^s \right) + f_{eBy}^s + f_{gBy}^s \end{cases} \tag{5}$$

3   Controller design

The AMB controller can be divided into three parts: driven mode of AMB and centralized controller. The centralized controller then contains nominal controller and robust compensator.

3.1   Driven mode of AMB

The driven mode of AMB refers to the realization of the expected AMB force. The differential driven mode is a traditional application in industrial AMBs, shown in Fig.2. In differential driven mode, the current in the magnet pole contains bias current i^0 and control current i^c. A pair of opposite magnet poles together control one degree of freedom (DOF). The current in this pair of opposite magnet poles share the same bias current and and inverse control current, which can be written as $i_{n1}=i_n^0 + i_n^c$, $i_{n2}=i_n^0 - i_n^c$. In one magnet pole, the electromagnetic force generated by the single pole of the magnetic bearing can be expressed as

$$f_p = k\frac{i^2}{s^2}, k = \frac{\mu_0 A N^2}{4} \cos\theta \tag{6}$$

where i is the current, s is the gap, μ_0 is the magnetic field constant in vacuum, N is the number of coils turns, A is the cross-section area of the pole and θ is the angle of the pole. In differential driven mode, the AMB force can be written as

$$f_{bn} = \frac{k(i_{n1})^2}{\left(s_0 - y_k^b\right)^2} - \frac{k(i_{n2})^2}{\left(s_0 + y_k^b\right)^2}, \quad n = Ax, Ay, Bx, By \tag{7}$$

4

The expected AMB force can be designed by linearizing (7) at the balance position and the bias current.

$$u_n = k_i i_n^c + k_x y_n^b$$
$$k_i = 4k\frac{i^0}{s_0^2}, \, k_x = 4k\frac{(i^0)^2}{s_0^3} \quad n = Ax, Ay, Bx, By$$
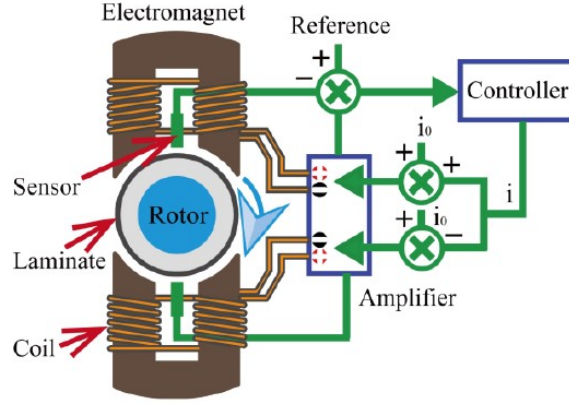
(8)

Figure 2: The differential driven mode of single DOF AMB-rotor system.

The framework of the differential driven mode in the controller can be described as Fig.3. In Fig.3, $G_c(s)$ refers to the transfer function of the centralized controller in each channel.
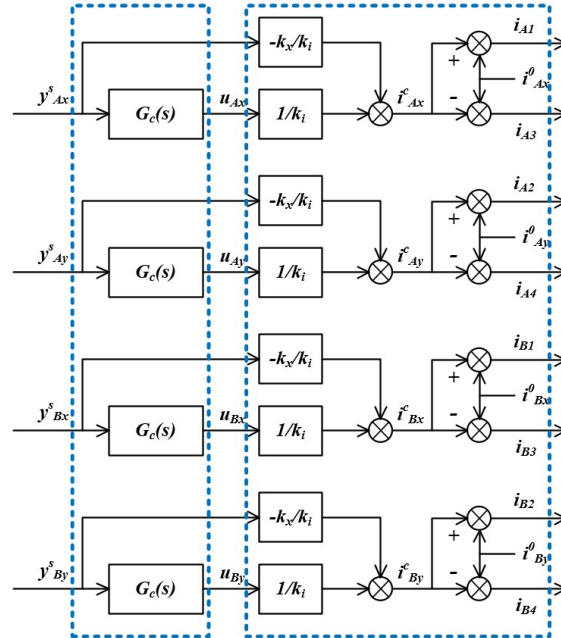

Figure 3: The framework of the differential driven mode in the controller.

3.2   Centralized controller

The centralized controller contains contains nominal controller and robust compensator. The framework of the centralized controller is shown in Fig.4. The nominal controller aims to stabilized the nominal system and the compensator aims to estimate the lumped uncertainties d according to the response signal y as well as the control signal u.
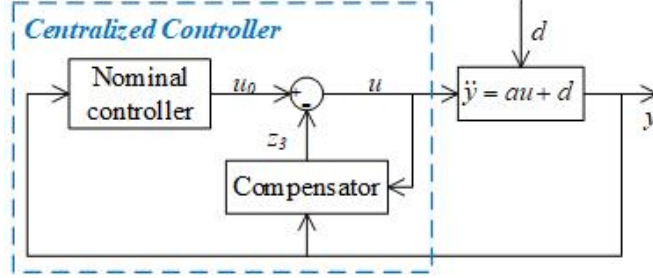

Figure 4: The framework of the centralized controller.

According to (4) and Fig.4, it is obvious that the nominal plant of the system is $ddoty = au$. In fact, proportional-differential (PD) form of nominal controller (shown in (9)) is enough to stabilize the nominal system.

$$G_n\left(s\right) = \frac{u_0\left(s\right)}{y\left(s\right)} = k_P + \frac{k_D s}{\tau_D s + 1} \tag{9}$$

As for compensator, it requires compensate the influence of lumped uncertainties. According to (4) and Fig.4, the plant with lumped uncertainties can be written as:

$$y\left(s\right) = \frac{a}{s^2} u\left(s\right) + \frac{1}{s^2} d\left(s\right) \tag{10}$$

The total control signal u is

$$u\left(s\right) = u_0\left(s\right) + v\left(s\right) \tag{11}$$

Taken (11) into (10), it obtains

$$y\left(s\right) = \frac{a}{s^2} G_n\left(s\right) y\left(s\right) + \frac{1}{s^2}\left[av\left(s\right) + d\left(s\right)\right] \tag{12}$$

Equation (12) indicates that the best choice to compensate the lumped uncertainties is

$$v^*\left(s\right) = -\frac{1}{a} d\left(s\right) = u\left(s\right) - \frac{s^2}{a} y\left(s\right) \tag{13}$$

However, (13) is a non-causal signal. Thus, a robust filter $F(s)$ is required and the compensation signal can be written as:

$$v\left(s\right) = F\left(s\right) v^*\left(s\right) \tag{14}$$

Taken $F(s)$ as

$$F\left(s\right) = \frac{\beta_3}{s^3 + \beta_1 s^2 + \beta_2 s + \beta_3} \tag{15}$$

6

Then, the compensator has a specific expression

$$v\left(s\right) = \frac{\beta_3}{s^3 + \beta_1 s^2 + \beta_2 s + \beta_3} u\left(s\right) - \frac{1}{a} \frac{\beta_3 s^2}{s^3 + \beta_1 s^2 + \beta_2 s + \beta_3} y\left(s\right) \tag{16}$$

The characteristics function of the compensator is

$$s^3 + \beta_1 s^2 + \beta_2 s + \beta_3 = 0 \tag{17}$$

To ensure the stability of the compensator, corresponding parameters can taken as

$$\beta_1 = 3\omega_0, \quad \beta_2 = 3\omega_0^2, \quad \beta_3 = \omega_0^3 \tag{18}$$

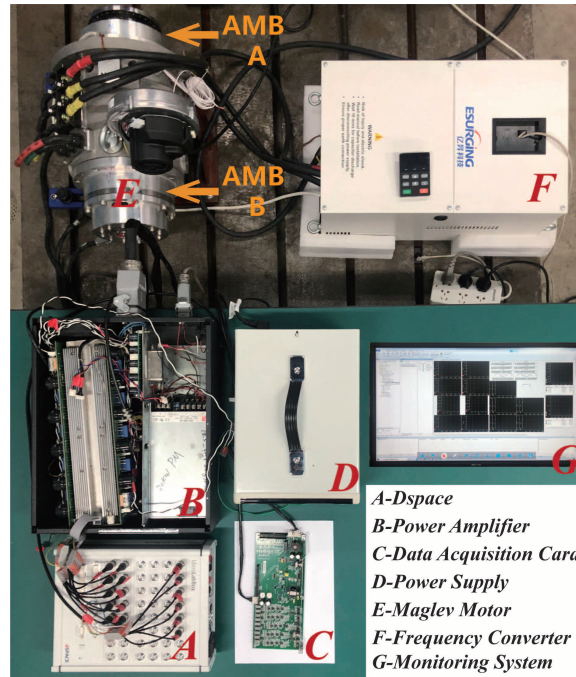# 4   Experimental verification

Figure 5: Description of the test rig.

In order to verify the effectiveness of the proposed control method, verification experiments are carried out on the magnetic bearing test rig. The experimental test rig for this study is a PMSM at Tsinghua University, pictured in Fig.5. The rotor of the test rig is 0.4866 m long with a total mass of 13.98 kg and is horizontally supported by two radial AMBs and one axial AMB. The radial clearance of the AMBs is 0.4 mm and the clearance of touchdown bearings is 0.2 mm. Radial and axial displacements of the rotor were measured using five inductive sensors. Ten current-controlled pulse width modulated amplifiers power the magnet coils to generate the expected bearing force.

The test rig works originally under a decentralized differential PID controller with a bias current of 2.5 A. This provides an open-loop bearing negative stiffness of 3.08×10^5 N/m and

a current gain of 49.34 N/A. The equivalent stiffness brought by the original PID controller is 2×10^5 N/m. For comparison, the PD parameter in the designed controller takes the same value as the original PID.

The displacement response at sensor of original PID controller and the proposed PD-Compensator controller at the rotating speed from 0 to 100 Hz (6000 r/min) are shown in Fig.6. In Fig.6, the peak value under PID appears at 37 Hz while that of PD-Compensator controller appears at 47 Hz. Besides, from 50 Hz to 70 Hz, the radius response under PD-Compensator controller is larger than that of PID. In fact, the performance of the compensator depends on filter $F(s)$. The crossover frequency of $F(s)$ was designed at 45 Hz in this test rig, which means the compensator will not compensate the unbalance force when the rotating speed is over 45 Hz. From another perspective, the compensator can be considered as a revision of equivalent stiffness and damping on the basis of PD controller. This indicates that compensator, in a way, enlarge the bearing stiffness below the crossover frequency and narrow it above the crossover frequency. In other words, compensator will not compensate the unbalance force any more in high frequency range and will not influence the realization of self-balance at high speed.

5   Conclusion

In view of the gyroscopic effect, the unbalance force, the unmodeled dynamics and disturbances in the rotor-AMBs system, a robust controller based on signal compensation was proposed in this study to increase the robustness of the controller.Firstly, a decentralized controller plant model was developed with lump uncertainties. On the basis of the model, the control system is designed. The control system contains nominal controllers and compensators. The target of the nominal controller is to stabilize the nominal part of the system. The robust compensator aims to generate the compensation signal to suppress the lumped uncertainties equivalent disturbance robustly. Corresponding experimental verification has been carried out on an industrial AMB-supported PMSM test rig. The proposed strategy is compared with a PID controller with the same nominal controller. The results show that the proposed control strategy is effective.

References

[1] Qi Chen, Gang Liu, and Bangcheng Han. Unbalance vibration suppression for ambs system using adaptive notch filter. *Mechanical Systems and Signal Processing*, 93:136–150, 2017.

[2] Qi Chen, Gang Liu, and Shiqiang Zheng. Suppression of imbalance vibration for ambs controlled driveline system using double-loop structure. *Journal of Sound and Vibration*, 337:1–13, 2015.

[3] Abhishek Dhyani, Manoj Kumar Panda, and Bhola Jha. Moth-flame optimization-based fuzzy-pid controller for optimal control of active magnetic bearing system. *Iranian Journal of Science and Technology, Transactions of Electrical Engineering*, 42(4):451–463, 2018.

[4] Jiancheng Fang, Xiangbo Xu, and Jinjin Xie. Active vibration control of rotor imbalance in active magnetic bearing systems. *Journal of vibration and control*, 21(4):684–700, 2015.

[5] Xudong Guan, Jin Zhou, Chaowu Jin, and Yuanping Xu. Disturbance suppression in active magnetic bearings with adaptive control and extended state observer. *Proceedings of the Institution of Mechanical Engineers, Part I: Journal of Systems and Control Engineering*, 234(2):272–284, 2019.

[6] Kejian Jiang and Changsheng Zhu. Multi-frequency periodic vibration suppressing in active magnetic bearing-rotor systems via response matching in frequency domain. *Mechanical Systems and Signal Processing*, 25(4):1417–1429, 2011.

[7] Chaowu Jin, Kaixuan Guo, Yuanping Xu, Hengbin Cui, and Longxiang Xu. Design of magnetic bearing control system based on active disturbance rejection theory. *Journal of Vibration and Acoustics*, 141(1), 2019.

[8] Z. Kai, J. Dong, X. Dai, and X. Zhang. Vibration control of a turbo molecular pump suspended by active magnetic bearings. *AMER SOC Mechanical Engineers*, pages 795–799, 2011.

[9] Chao Liu, Gang Liu, and Jiancheng Fang. Feedback linearization and extended state observer-based control for rotor-ambs system with mismatched uncertainties. *IEEE Transactions on Industrial Electronics*, 64(2):1313–1322, 2017.

[10] Hai Rong and Kai Zhou. Nonlinear zero-bias current control for active magnetic bearing in power magnetically levitated spindle based on adaptive backstepping sliding mode approach. *Proceedings of the Institution of Mechanical Engineers, Part C: Journal of Mechanical Engineering Science*, 231(20):3753–3765, 2016.

[11] Gerhard Schweitzer and Eric H Maslen. Magnetic bearings. theory, design, and application to rotating machinery. 2009.

[12] R. Siva Srinivas, R. Tiwari, and Ch Kannababu. Application of active magnetic bearings in flexible rotordynamic systems – a state-of-the-art review. *Mechanical Systems and Signal Processing*, 106:537–572, 2018.

[13] Te-Jen Su, Wen-Pin Kuo, Van-Nam Giap, H Quan Vu, and Quang-Dich Nguyen. Active magnetic bearing system using pid-surface sliding mode control. In *2016 Third International Conference on Computing Measurement Control and Sensor Network (CMCSN)*, pages 5–8. IEEE.

[14] Weiyu Zhang and Huangqiu Zhu. Radial magnetic bearings: An overview. *Results in Physics*, 7:3756–3766, 2017.
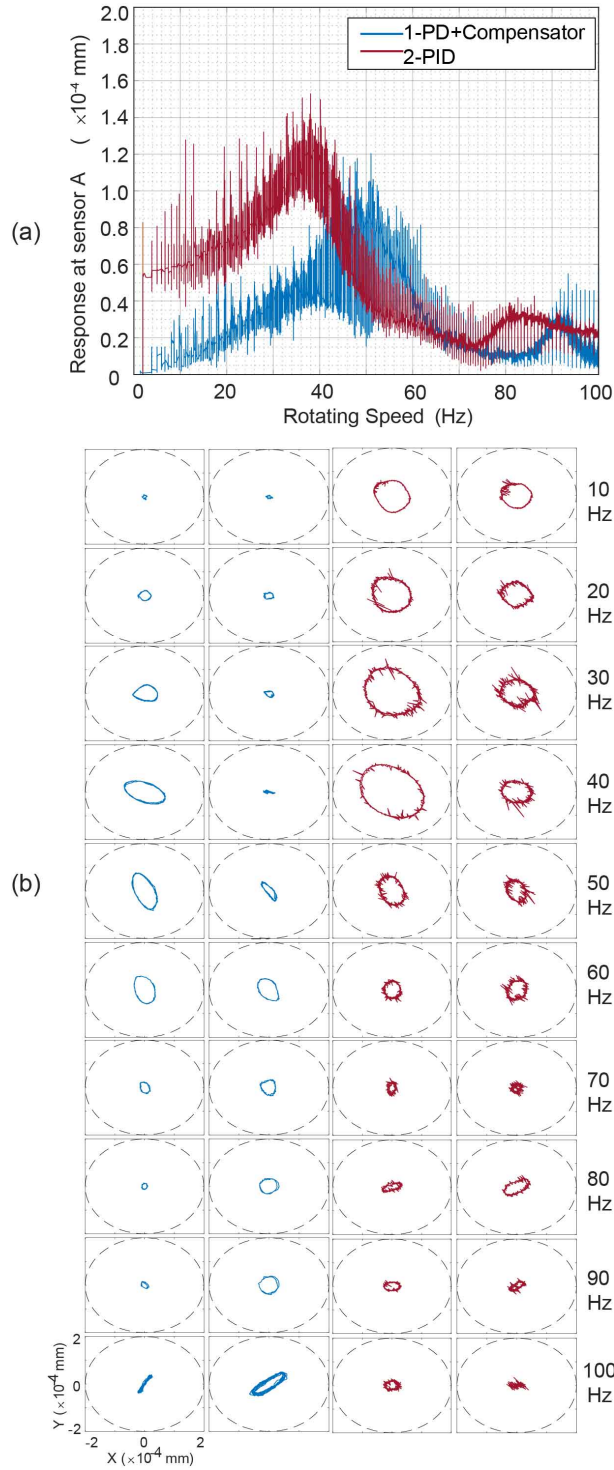
Figure 6: Response of the original PID controller from 0 to 100 Hz. (a) Displacement response at sensor A (b) Rotor trajectory at AMB A and AMB B during different rotating speed.